SCIENCE CHINA
Information Sciences

• RESEARCH PAPER •

May 2023, Vol. 66 152302:1–152302:11
https://doi.org/10.1007/s11432-022-3555-y

Clipping discrete multi-tone for peak-power-constraint IM/DD optical systems

Ji ZHOU[1*], Liangchuan LI[2*], Jiale HE[2], Xiaofeng LU[2], Yu BO[2], Guanyu WANG[2], Yuanda HUANG[2], Gengchen LIU[2], Yanzhao LU[2], Shecheng GAO[1*], Yuanhua FENG[1], Shancheng ZHAO[1], Weiping LIU[1], Changyuan YU[3] & Zhaohui LI[4,5]

[1]*Department of Electronic Engineering, College of Information Science and Technology, Jinan University, Guangzhou* 510632*, China;*
[2]*Optical Research Department, Huawei Technologies Co., Ltd., Dongguan* 523808*, China;*
[3]*Department of Electronic and Information Engineering, The Hong Kong Polytechnic University, Hong Kong* 999077*, China;*
[4]*Guangdong Provincial Key Laboratory of Optoelectronic Information Processing Chips and Systems, Sun Yat-sen University, Guangzhou* 510275*, China;*
[5]*Southern Marine Science and Engineering Guangdong Laboratory (Zhuhai), Zhuhai* 511458*, China*

Received 11 February 2022/Revised 27 May 2022/Accepted 22 July 2022/Published online 20 April 2023

Abstract High peak-to-average power ratio (PAPR) is a major drawback of discrete multi-tone (DMT) in peak-power-constraint (PPC) intensity-modulation/direct-detection (IM/DD) optical systems. Symmetric clipping operation is a frequently-used and practical method for mitigating the PAPR of the DMT signal. However, clipping noise is inevitably induced by the symmetric clipping operation, thereby deteriorating the system's performance. In this paper, we study the statistical characteristics of the clipping noise in detail. Depending on the statistical characteristics, clipping-noise-cancellation (CNC) algorithms are proposed to mitigate the clipping noise in the clipping DMT systems. Theoretically, the clipping noise can be completely removed using the low-density-parity-check-assisted CNC algorithm (LDPC-assisted CNC algorithm). To verify the superiority of the clipping DMT with the CNC algorithm, we conduct an experiment with a 50 Gb/s DMT system using 10G-class commercial devices for the scenario of PPC passive optical networks. The receiver sensitivity of the clipping DMT system with the CNC algorithm can reach −24 dBm at a 20% soft-decision forward-error-correction limit, which is 2.5 dB higher than that of the DMT system without clipping operation. The clipping operation and the CNC algorithm are added after the original digital signal processing, thereby demonstrating the potential to effectively overcome the drawback in DMT signals and other high-PAPR signals.

Keywords discrete multi-tone, peak-to-average power ratio, peak-power constraint, clipping-noise cancellation, intensity-modulation/direct-detection optical systems

Citation Zhou J, Li L C, He J L, et al. Clipping discrete multi-tone for peak-power-constraint IM/DD optical systems. Sci China Inf Sci, 2023, 66(5): 152302, https://doi.org/10.1007/s11432-022-3555-y

1 Introduction

Intensity-modulation/direct-detection (IM/DD) optical systems are promising technologies for the short-reach scenarios of optical interconnects, passive optical networks, and mobile fronthaul networks owing to their low cost, small footprint and low power consumption [1–3]. An optical amplifier is unnecessary for the short-reach IM/DD optical systems. Therefore, the IM/DD optical systems without the optical amplifier can be considered peak-power-constraint (PPC) systems [4–6]. In the PPC IM/DD optical systems, the main noise results from the transceivers, and the average power of the transmitted signal determines the signal-to-noise ratio (SNR) of the received signal. A high peak-to-average power ratio (PAPR) leads to the low average power of the modulated signal and thus low SNR of the received signal, which is the main obstacle to achieve a high receiver sensitivity in the PPC IM/DD optical systems [7–9].

* Corresponding author (email: zhouji@jnu.edu.cn, liliangchuan@huawei.com, gaosc825@163.com)

Discrete multi-tone (DMT) is a popular multi-carrier modulation for the cost-sensitive and bandwidth-limited IM/DD optical systems [10–12]. Owing to the bit and power allocations, the DMT signal exhibits high spectral efficiency, flexible data rate, and high robustness to the spectral distortions. High-speed DMT systems have been implemented in several scenarios, including passive optical networks (PONs), optical interconnects and mobile fronthaul networks [13–15]. However, compared to the single-carrier signal, the DMT signal has a higher PAPR, thereby limiting its performance in the PPC IM/DD optical systems [16–18]. The main drawbacks of the high PAPR are as follows. (1) The high-PAPR signals have limited amplitudes in the PPC IM/DD optical systems, thereby causing low average power, and thus low SNR. (2) A higher PAPR indicates a higher quantizing noise due to the limited quantization bits of digital-to-analog converter (DAC) and analog-to-digital converter (ADC). In other words, the high-PAPR DMT signal requires DAC and ADC with high quantization bits. Therefore, a PAPR reduction is crucial for the DMT signal in the PPC IM/DD optical systems.

For the PAPR reduction, several methods have been widely studied [19–22], including partial transmit sequence technique, exponential companding technique, clipping operation, and spreading technique. Among these, the clipping operation was proposed to cut the peak of the DMT signal, a straightforward and practical method to reduce the PAPR [23–25]. However, the clipping noise is inevitably induced by the clipping operation, thereby undoubtedly deteriorating the performance of the DMT systems. Therefore, an optimal clipping ratio must be selected to balance the PAPR reduction and the clipping noise in the clipping DMT signal. If the clipping noise can be removed, the performance of the clipping DMT system can be further improved. In this paper, we will study the theoretical characteristics of the clipping DMT signal in the PPC IM/DD optical systems and propose an effective clipping-noise cancellation (CNC) algorithm for mitigating the clipping noise.

The main contributions of this paper are as follows.

- The PAPR, clipping noise, and effective SNR are theoretically analyzed for the clipping DMT signal. Based on the theoretical analyses, we propose the CNC algorithm for effectively mitigating the clipping noise to improve the performance of the clipping DMT system. The proposed scheme does not change the original structure of the digital signal processing (DSP), and is applicable in reducing the PAPR for other high-PAPR signals.
- To verify the benefits of clipping DMT with CNC algorithm, we conduct an experiment with 50 Gb/s DMT system using 10G-class commercial devices for the scenario of PPC PONs. At the 20% forward-error-correct (FEC) limit, the receiver sensitivity of the clipping DMT system with the CNC algorithm is 2.5 dB higher than that of DMT without the clipping operation.

The remainder of this paper is organized as follows. In Section 2, the statistical characteristics of DMT are analyzed in detail. In Section 3, the CNC algorithm is proposed for mitigating the clipping noise. The simulations are constructed to verify the theoretical analyses and the feasibility of the CNC algorithm. In Section 4, the experimental setups are introduced and the experimental results are analyzed. Finally, the paper is concluded in Section 5.

2 Statistical characteristics of DMT

In this section, the statistical characteristics of the clipping DMT signal are analyzed to provide a theoretical basis for the CNC algorithm. In the previous studies, the statistical characteristics of the DMT signal with asymmetric clipping operation have been widely studied [26–28]. Different from the asymmetric clipping operation, the symmetric clipping operation is applied to reduce the PAPR of the DMT signal. We will investigate the clipping distortions and effective SNR in the DMT signal with symmetric clipping operation.

2.1 Clipping distortions

Based on the central-limit theorem, the DMT signal can be modeled as Gaussian distribution. The probability density function (PDF) of the DMT signal can be defined as

$$N(x;\mu,\sigma^2)=\frac{1}{\sqrt{2\pi}\sigma}\mathrm{e}^{-\frac{(x-\mu)^2}{2\sigma^2}}, \tag{1}$$

where x is the DMT signal. μ is the mean of the DMT signal, which is usually equal to zero. σ^2 is the average power of the DMT signal. The symmetric clipping operation for the DMT signal is defined as

$$x_c = \begin{cases} A, & x > A, \\ x, & |x| \leqslant A, \\ -A, & x < -A, \end{cases} \tag{2}$$

where A is the clipping amplitude. The clipping ratio can be defined as $10 \times \log_{10}(\eta^2)$ where η is equal to A/σ. Therefore, the PDF of the clipping DMT signal can be expressed as

$$\mathrm{PDF}_c(x) = \begin{cases} N(x;\ 0,\ \sigma^2), & |x| \leqslant A, \\ Q(\eta)\delta(|x| - A),\ |x| > A, \end{cases} \tag{3}$$

where $Q(\eta) = \int_{\eta}^{\infty} \frac{1}{\sqrt{2\pi}} \mathrm{e}^{-\frac{x^2}{2}} \mathrm{d}x$. $\delta(\cdot)$ is the Dirac delta function with an unit impulse. According to the PDF of the clipping DMT signal, the average power of the DMT signal with clipping operation can be calculated by

$$\begin{aligned} E(x_c^2) &= \int_{-\infty}^{\infty} x_c^2 \times \mathrm{PDF}(x_c)\mathrm{d}x \\ &= 2A^2Q(\eta) + \int_{-A}^{A} x^2 \frac{1}{\sqrt{2\pi}\sigma} \mathrm{e}^{-\frac{x^2}{2\sigma^2}} \mathrm{d}x \\ &= 2A^2Q(\eta) + \sigma^2 \left[1 - 2Q(\eta) - \frac{2\eta}{\sqrt{2\pi}} \mathrm{e}^{-\frac{\eta^2}{2}}\right] \\ &= \sigma^2 \left[1 + 2\eta^2 Q(\eta) - 2Q(\eta) - \frac{2\eta}{\sqrt{2\pi}} \mathrm{e}^{-\frac{\eta^2}{2}}\right] \\ &= \sigma^2 \times N(\eta), \end{aligned} \tag{4}$$

where $N(\eta) = [1 + 2\eta^2 Q(\eta) - 2Q(\eta) - \frac{2\eta}{\sqrt{2\pi}} \mathrm{e}^{-\frac{\eta^2}{2}}]$. As a result, the PAPR of the clipping DMT signal can be calculated by

$$\mathrm{PAPR} = A^2/E(x_c^2) = \eta^2/N(\eta). \tag{5}$$

Obviously, the symmetric clipping operation can effectively reduce the PAPR of the DMT signal. However, the time-domain symmetric clipping operation induces the distortions on the frequency-domain subcarriers. The clipping distortions can be decomposed into an attenuation $K(\eta)$ and additive clipping noise $N_c(\eta)$. After the symmetric clipping operation, the signal X_c on the frequency-domain subcarriers can be defined as

$$X_c = K(\eta) \times X + N_c(\eta), \tag{6}$$

where X is the signal on the frequency-domain subcarriers before the symmetric clipping operation. The attenuation $K(\eta)$ can be calculated by

$$\begin{aligned} K(\eta) &= \frac{E(x_c x)}{E(x^2)} \\ &= \frac{2\int_A^{\infty} Ax \frac{1}{\sqrt{2\pi}\sigma} \mathrm{e}^{-\frac{x^2}{2\sigma^2}} \mathrm{d}x + \int_{-A}^{A} x^2 \frac{1}{\sqrt{2\pi}\sigma} \mathrm{e}^{-\frac{x^2}{2\sigma^2}} \mathrm{d}x}{\sigma^2} \\ &= \frac{2\eta}{\sqrt{2\pi}} \mathrm{e}^{-\frac{\eta^2}{2}} + 1 - 2Q(\eta) - \frac{2\eta}{\sqrt{2\pi}} \mathrm{e}^{-\frac{\eta^2}{2}} \\ &= 1 - 2Q(\eta). \end{aligned} \tag{7}$$

The attenuation $K(\eta)$ can be easily mitigated by the normalization. The variance of additive clipping noise $N_c(\eta)$ can be calculated by

$$\sigma_{N_c}^2 = E(X_c^2) - E[K^2(\eta)X^2] = \sigma^2 \times [N(\eta) - K^2(\eta)]. \tag{8}$$

Figure 1 shows the PAPR (blue circle) and clipping noise (orange triangle) versus clipping ratio for the clipping DMT signal. The PAPR of the DMT signal is set to 12 dB before the symmetric clipping operation. When the clipping ratio is set to 12 dB, the PAPR is still 12 dB due to the inactive symmetric clipping operation. Then, the PAPR decreases with the decrease of the clipping ratio. When the clipping ratio is set to 2 dB, the PAPR is equal to approximately 3.8 dB. Therefore, the symmetric clipping operation can effectively reduce the PAPR of the DMT signal. However, the symmetric clipping operation induces the clipping noise, which increases with the decrease of the clipping ratio. Obviously, the performance of the clipping DMT system is sensitive to the clipping ratio. Therefore, we should choose a suitable clipping ratio for the clipping DMT system.

2.2 Effective SNR

In fact, the peak of the DMT signal cannot achieve the value of ∞. The peak of the DMT signal is equal to the value of A_p under the average power of σ^2. Therefore, the PAPR_0 of the DMT signal can be defined as A_p^2/σ^2, which denotes the PAPR of the DMT signal without symmetric clipping operation. We assume that A_p is the peak constraint in the PPC IM/DD optical systems. The amplitude of the clipping DMT signal can be amplified to the range of $[-A_p\ A_p]$ with the gain of α, which can be expressed as

$$\alpha = A_p/A = \sqrt{\frac{\mathrm{PAPR}_0}{\eta^2}}. \tag{9}$$

The average power of the amplified clipping DMT signal can be calculated by

$$P_s = \alpha^2 \times E[K^2(\eta)X^2]. \tag{10}$$

The main noise in the clipping DMT system contains the clipping noise and the white noise. Meanwhile, the clipping noise and white noise are uncorrelated. Therefore, the total noise power is approximately equal to

$$P_n = \alpha^2 \times \sigma_{N_c}^2 + \sigma_N^2, \tag{11}$$

where σ_N^2 is the power of white noise. Therefore, the effective SNR of the clipping DMT system can be calculated by

$$\begin{aligned}\mathrm{SNR_E} &= \frac{\alpha^2 \times E[K^2(\eta)X^2]}{\alpha^2 \times \sigma_{N_c}^2 + \sigma_N^2} = \frac{\alpha^2 K^2(\eta)\sigma^2}{\alpha^2\sigma_{N_c}^2 + \sigma_N^2} \\ &= \frac{\mathrm{PAPR}_0 \times K^2(\eta) \times \mathrm{SNR}}{\mathrm{PAPR}_0 \times [N(\eta) - K^2(\eta)] \times \mathrm{SNR} + \eta^2},\end{aligned} \tag{12}$$

where SNR denotes the SNR of the DMT without symmetric clipping operation, which is equal to σ^2/σ_N^2.

Figure 2 shows the effective SNR ($\mathrm{SNR_E}$) versus the clipping ratio (η) for different SNR under the PAPR_0 of 12 dB. When the clipping ratio is set to 12 dB, the symmetric clipping operation is not valid and the effective SNR is equal to the SNR. With the decrease of the clipping ratio, the effective SNR increases at the beginning owing to the increase of average signal power, and then decreases due to the increase of the clipping noise. Therefore, the symmetric clipping operation can make the DMT signal achieve the highest effective SNR under an optimal clipping ratio. The optimal clipping ratio depends on the balance among the white-noise power, the clipping-noise power, and average-signal power. When the SNR increases, the white-noise power decreases, and the clipping-noise power plays a dominant role, and the clipping ratio should be increased to decrease the clipping-noise power for making sure the increased effective SNR. As a result, the optimal clipping ratios are different under the different SNRs. From the above analyses, the clipping noise is the main obstacle to further improve the performance of the clipping DMT systems. Fortunately, Eq. (6) demonstrates that the clipping noise is additive to the frequency-domain signal. Therefore, if we can accurately estimate the clipping noise, the clipping noise can be effectively mitigated in theory.

3 Clipping-noise cancellation

In this section, we will propose the CNC algorithm based on the theoretical characteristics of the clipping noise for the clipping DMT systems. The simulation is set up to study the performance of the proposed algorithms in the clipping DMT systems.

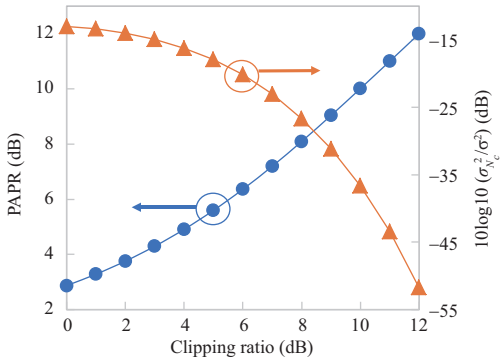

Figure 1 (Color online) The PAPR (blue circle) and clipping noise (orange triangle) versus clipping ratio for the clipping DMT signal.

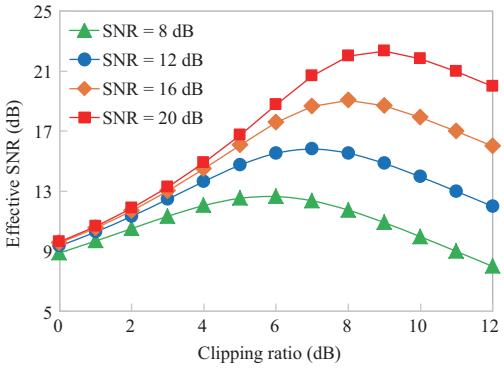

Figure 2 (Color online) Effective SNR versus the clipping ratio for different SNRs under the PAPR_0 of 12 dB.

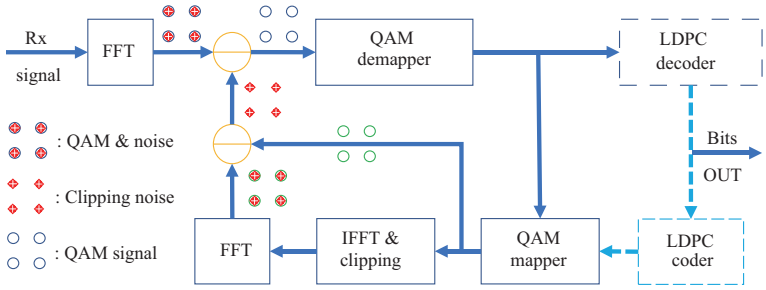

Figure 3 (Color online) Schematic diagram of the CNC algorithms for the clipping DMT systems.

Figure 3 depicts the schematic diagram of the CNC algorithms for the clipping DMT systems. The received signal is first sent into the fast Fourier transform (FFT) to obtain the quadrature amplitude modulation (QAM) signal with the clipping noise. The QAM signal can be normalized to remove the attenuation $K(\eta)$ in (6). The normalized QAM signal with the clipping noise can be expressed as $X'_c = X + N'_c$ where N'_c is equal to $N_c(\eta)/K(\eta)$. After the QAM demapper, the recovered bits have a part of errors due to the clipping noise, white noise, and channel distortions. In theory, the clipping noise can be estimated accurately by using the noise reconstruction when the bit error ratio (BER) is within an acceptable range. The decision-assisted CNC algorithm was proposed to reconstruct and remove the clipping noise [29]. In the decision-assisted CNC algorithm, the recovered bits after the QAM demapper are sent into the QAM mapper to regenerate the QAM signal $\hat{X}$. Then, the clipping DMT signal is regenerated after the inverse fast Fourier transform (IFFT) and clipping operation. The clipping operation in the CNC algorithm should use the same clipping ratio of the clipping operation at the transmitter end. After the FFT, the QAM signal with clipping noise subtracts the QAM signal $\hat{X}$ to estimate the clipping noise $\hat{N}_c$. It is worth noting that the clipping noise can be estimated from the corresponding DMT symbol with no need for the other symbols. Finally, the X'_c subtracts the estimated clipping noise $\hat{N}_c$ to recover more clear QAM signal. When the estimated clipping noise is more accurate, the recovered QAM signal is more accurate and the BER of the recovered bits is lower. The accuracy of the estimated clipping noise in turn depends on the BER of the recovered bits. Therefore, there must be an optimal clipping ratio for the balance between the clipping noise and the BER.

We propose low-density-parity-check (LDPC)-assisted CNC algorithm to estimate and remove the clipping noise more accurately than decision-assisted CNC algorithm. The similar algorithm was used to eliminate inter-carrier interference for non-orthogonal DMT in our previous work [30]. In the LDPC-assisted CNC algorithm, we employ the LDPC to correct the error bits for estimating the more-accurate clipping noise. The dash boxes and lines in Figure 3 depict the additional processes in the LDPC-assisted CNC algorithm. The output bits of the QAM demapper are sent into the LDPC decoder for correcting the error bits. In general, when the BER is less than the limit of 0.027 before the LDPC decoder, the LDPC with 20% overhead can correct all the error bits to achieve the BER of near zero. After the LDPC decoder, the corrected bits are sent into the LDPC coder again to obtain LDPC-coded bits. Then, the

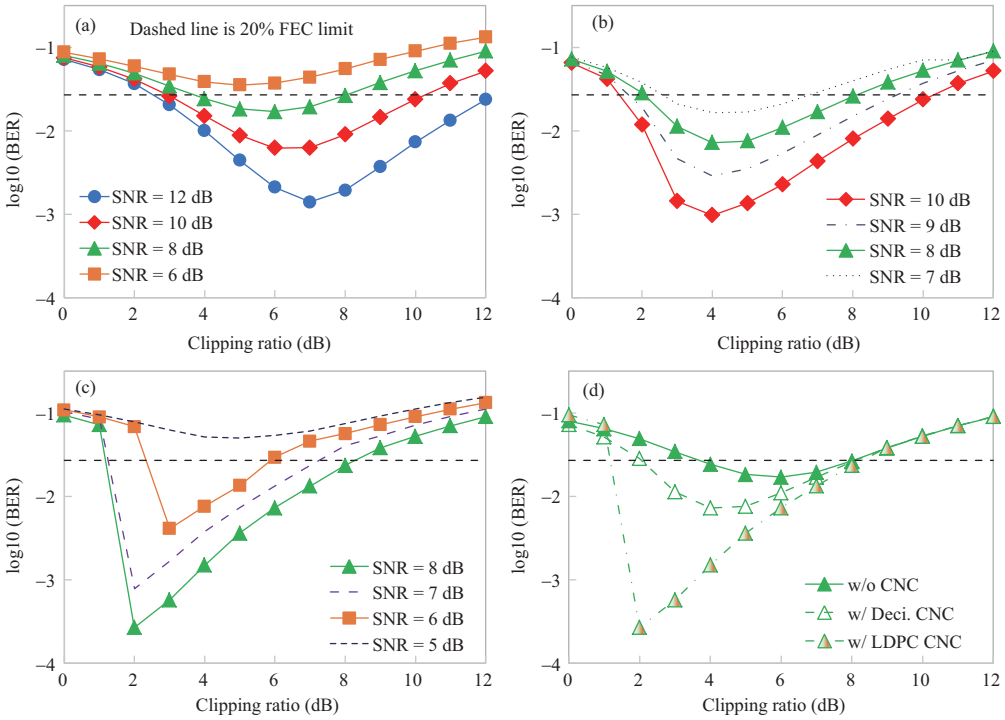

Figure 4 (Color online) BER versus the clipping ratio for the clipping DMT system (a) without CNC algorithm, (b) with decision-assisted CNC algorithm, (c) with LDPC-assisted CNC algorithm, and (d) performance comparison between clipping DMT system without CNC algorithm and with decision-assisted (Deci.) CNC algorithm and LDPC-assisted CNC algorithm when the SNR is set to 8 dB.

following processes are similar to that of the decision-assisted CNC algorithm. It is worth noting that the LDPC has a trigger effect to correct the error bits. The LDPC starts to correct the error bits when the BER before LDPC is lower than the triggered value, which is usually equal to approximate 0.035 for the LDPC with 20% overhead. However, when the BER before LDPC is higher than the triggered value, the BER after LDPC is higher than that before LDPC. Therefore, the LDCP assistance is effective for CNC algorithm only when the BER is lower than triggered value, which can obtain a considerable benefit. However, when the BER is higher than the triggered value, the error propagation appears in the LDPC-assisted CNC algorithm, which seriously degrades the BER performance. In order to relieve the error propagation, before the LDPC assistance, a decision-assisted CNC algorithm can be added to reduce the BER for reaching the triggered value.

Next, we set up a simulation to verify the feasibility of the clipping DMT system with the CNC algorithm. In the simulation, the IFFT/FFT size is set to 1024. 16QAM is modulated on each subcarrier. The LDPC is the soft-decision mode and its overhead is set to 20%. The peak constraint is set to 0.15. Under this peak constraint, the noise power is set to the 2.07×10^{-4} to achieve the SNR of 8 dB for the DMT signal. We can change the noise power to adjust the SNR of the DMT signal. Figure 4(a) shows the BER versus the clipping ratio for the clipping DMT signal without CNC algorithm. The PAPR of the DMT frame without the clipping operation is approximately 12 dB. Therefore, when the clipping ratio is larger than 12 dB, the clipping operation does not work to decrease the PAPR. With the decrease of the clipping ratio less than 12 dB, the BER decreases at the beginning and then increases, which coincides with the trend of the effective SNR shown in Figure 2. The optimal clipping ratios for the clipping DMT system are 6 and 7 dB for the SNRs of 8 and 12 dB, respectively. Obviously, the simulation results match well with the theory results in Section 2.

Figure 4(b) depicts the BER versus the clipping ratio for the clipping DMT system with decision-assisted CNC algorithm. The decision-assisted CNC algorithm can eliminate a part of clipping noise to improve the performance of the clipping DMT system. At the 20% soft-decision forward-error-correction (SD-FEC) limit, the required SNR of the clipping DMT system with the decision-assisted CNC algorithm is approximately 1 dB lower than that without CNC algorithm. At the BER of 10^{-3}, the required SNR of the clipping DMT system with decision-assisted CNC algorithm is approximately 2 dB lower than that without CNC algorithm. Therefore, the clipping DMT with the decision-assisted CNC algorithm has

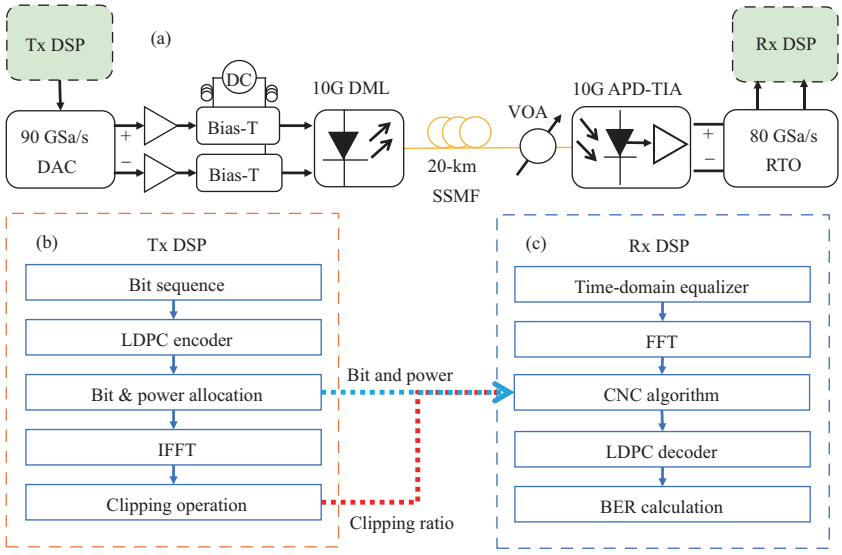

Figure 5 (Color online) (a) Experimental setups of 50 Gb/s DMT system using 10G-class commercial devices; (b) block diagram of Tx DSP; (c) block diagram of Rx DSP.

better performance compared to the clipping DMT without the CNC algorithm.

Figure 4(c) depicts the BER versus the clipping ratio for the clipping DMT system with LDPC-assisted CNC algorithm. The LDPC-assisted CNC algorithm has the potential to eliminate the clipping noise completely, which can further improve the performance of the clipping DMT system. At the 20% SD-FEC limit, the required SNR of the clipping DMT system with LDPC-assisted CNC algorithm is >2 dB lower than that without CNC algorithm. At the BER of 10^{-3}, the required SNR of the clipping DMT system with LDPC-assisted CNC algorithm is >5 dB lower than that without CNC algorithm. The LDPC-assisted CNC algorithm can deal with more clipping noise when the DMT system has a higher SNR. Therefore, the optimal clipping ratio of the clipping DMT system with LDPC-assisted CNC algorithm decreases with the increase of the SNR, which is contrary to that without CNC algorithm. When the clipping ratio is less than the optimal value, larger clipping noise makes the BER before the LDPC-assisted CNC algorithm higher than the triggered BER. The high BER before the LDPC-assisted CNC algorithm leads to the inaccurate estimated clipping noise. Due to the inaccurate estimated clipping noise, the BER after the LDPC-assisted CNC algorithm is higher than that before the LDPC-assisted CNC algorithm, which is known as the error propagation.

Figure 4(d) shows the performance comparison between the clipping DMT system without CNC algorithm, and with decision-assisted CNC algorithm and LDPC-assisted CNC algorithm when the SNR is set to 8 dB. When the SNR is set to 8 dB, the optimal clipping ratios are 6, 4 and 2 dB for the clipping DMT system without CNC algorithm, and with decision-assisted CNC algorithm and LDPC-assisted CNC algorithm, respectively. The LDPC-assisted CNC algorithm can mitigate a mass of clipping noise so that a large-scale clipping operation can be applied to the DMT signal. The BER of the clipping DMT system with LDPC-assisted CNC algorithm is two orders and more than one order of magnitude lower than that without CNC algorithm and with decision-assisted CNC algorithm, respectively. Obviously, the LDPC-assisted CNC algorithm has the better performance than the decision-assisted CNC algorithm. In Sections 4 and 5, the CNC algorithm denotes the LDPC-assisted CNC algorithm if there is no statement.

4 Experimental setups and results

In this section, we set up an experiment of 50 Gb/s DMT system using 10G-class commercial devices for the scenario of the passive optical network to demonstrate the performance of the clipping DMT with the CNC algorithm.

Figure 5(a) shows the experimental setup of the 50 Gb/s DMT system using low-cost 10G-class commercial devices. At the transmitter end, the digital DMT signal was generated by offline Tx DSP using MATLAB. The block diagram of the Tx DSP is depicted in Figure 5(b). The random bit sequence was firstly encoded by the LDPC encoder with 20% overhead. After interleaving operation, bit and power

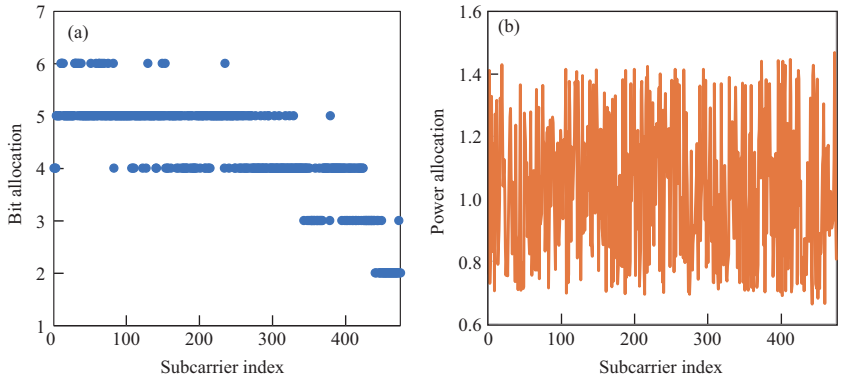

Figure 6 (Color online) (a) Bit allocation and (b) power allocation for the clipping DMT system with the CNC algorithm when the clipping ratio is set to 2 dB.

allocations were implemented based on the estimated SNR of the subcarrier for generating the QAM with the corresponding constellation order and power coefficient. Figure 6 shows the (a) bit allocation and (b) power allocation for the clipping DMT system with the CNC algorithm when the clipping ratio is set to 2 dB. The indices of the valid subcarriers are from 1 to 475 and the range of the allocated bits is from 6 to 2. Meanwhile, the relative power coefficients are round 1. When the power coefficients are larger (smaller) than 1, the allocated bits are more (less) than the bits directly calculated by the estimated SNR. Then, the QAM symbols based on the bit and power allocations were fed into IFFT with size of 1024 to generate the digital DMT signal. Finally, the peaks of the DMT signal were clipped depending on the clipping ratio.

The DAC converted the digital DMT signal into an analogue electrical signal, which has a maximum sampling rate of 90 GSa/s and a 3 dB bandwidth of 16 GHz. After a resampling operation, the sampling rate of the analogue electrical signal is 25 GSa/s. The link rate of DMT is 50 Gb/s when the average targeted bit number per sample is set to 2. An electrical amplifier (Microsemi OA3MHQM) was employed to amplify the analogue electrical signal. Then, the amplified electrical signal was modulated on 1330 nm optical carrier to generate an optical DMT signal by a commercial transmitter optical subassembly (TOSA) based on a 10G direct-modulated laser (DML). Finally, the optical DMT signal was launched into 20 km standard single-mode fiber (SSMF).

At the receiver end, we employed a variable optical attenuator (VOA) to change the received optical power (ROP). A commercial receiver optical sub-assembly (ROSA) based on 10G avalanche photodiodes (APD) with a 25G trans-impedance amplifier (TIA) was used to convert the optical signal into an electrical signal. Then, the electrical signal was digitized by an 80 GSa/s real-time oscilloscope (RTO) with a cutoff frequency of 36 GHz. Finally, the offline Rx DSP at the receiver end as indicated in Figure 5(c) was used to recover the digital signal into the transmitted bits. The Rx DSP should share the parameters of bit allocation, power allocation, and clipping ratio from the Tx DSP. The offline Rx DSP consists of a time-domain equalizer for compensating the linear and nonlinear distortions and the CNC algorithm for reducing the clipping noise. The main processing of the CNC algorithm has been detailed in Section 3.

Figure 7 shows the optimal clipping ratio versus the ROP for the clipping DMT system with or without CNC algorithm. The dashed line denotes the PAPR of the DMT frame without clipping operation, which is equal to approximately 12.7 dB. The optimal clipping ratio is set to achieve the highest effective SNR for the clipping DMT system. As Eq. (12) shows, the effective SNR depends on the white-noise power, clipping-noise power and average-signal power in the clipping DMT system. When the clipping DMT system without CNC algorithm has a high ROP, the white-noise power is relatively low, and the clipping-noise power plays a dominant role. The optimal clipping ratio should be high to reduce the clipping-noise power for improving the effective SNR. Therefore, for the clipping DMT system without CNC algorithm, the optimal clipping ratio increases from 6 to 12 dB with increase of ROP from −24.5 to −17 dBm, gradually approaching to the PAPR of the DMT signal without clipping operation. This tendency coincides with the theoretical and simulated analyses. In the clipping DMT system with the CNC algorithm, the clipping noise is effectively eliminated to obtain high effective SNR. Therefore, the optimal clipping ratio in the clipping DMT system with the CNC algorithm is much lower than that without the CNC algorithm. When the ROP is larger than −22 dBm, the optimal clipping ratio is set to 2 dB. However, the ability of the CNC algorithm descends with the decrease of ROP due to the

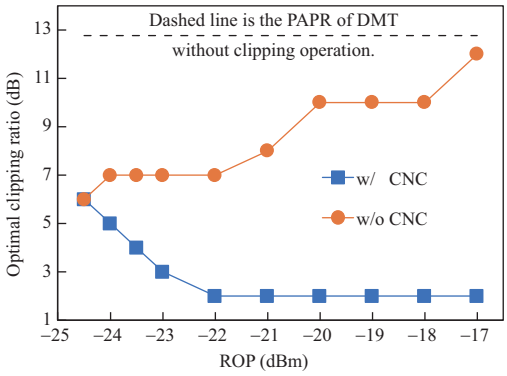

Figure 7 (Color online) Optimal clipping ratio versus the ROP for the clipping DMT system with or without the CNC algorithm.

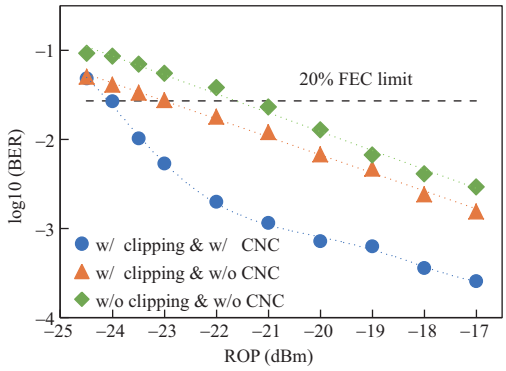

Figure 8 (Color online) BER versus ROP for 50 Gb/s DMT system w/ or w/o clipping operation and w/ or w/o CNC algorithm.

deteriorated BER. When the ROP is lower than −22 dBm and the optimal clipping ratio is set to 2 dB, the clipping noise cannot be removed completely by the CNC algorithm. The clipping ratio should be set to the value higher than 2 dB for ensuring low clipping noise and high effective SNR. Therefore, for the clipping DMT system with CNC algorithm, the optimal clipping ratio decreases from 6 to 2 dB with increase of ROP from −24.5 to −22 dBm. In conclusion, the optimal clipping ratios for the clipping DMT systems with and without CNC algorithm have two opposite developing trends.

Figure 8 depicts the BER versus ROP for the DMT system w/ or w/o clipping operation and w/ or w/o CNC algorithm. When the ROP is higher or equal to −22 dBm, the optimal clipping ratio is set to 2 dB, and the BER of the clipping DMT system with CNC algorithm is lower than 7% hard-decision FEC limit of 0.0038. Under this BER, the receiver sensitivity of the clipping DMT system with CNC algorithm is 5 dB and >5 dB higher than that of the clipping DMT system without CNC algorithm and DMT system without clipping operation. When the ROP is lower than −22 dBm, the clipping ratio should be increased to reduce the clipping noise for making sure the BER still lower than triggered value of the CNC algorithm. However, the increased clipping ratio reduces the gain of the clipping operation in the clipping DMT system with CNC algorithm. Therefore, the BER of the clipping DMT system with CNC algorithm deteriorates faster than that without clipping operation when the ROP is lower than −22 dBm. When the clipping operation is not employed, the ROP of the DMT system is approximate −21.5 dBm at the 20% SD-FEC limit. When the CNC algorithm is not employed, the ROP of the clipping DMT system is approximately −23 dBm at the 20% SD-FEC limit. When the CNC algorithm is employed, the ROP of the clipping DMT system is approximately −24 dBm at the 20% SD-FEC limit. Therefore, the receiver sensitivity of the clipping DMT system with CNC algorithm is 1 and 2.5 dB higher than that of the clipping DMT system without CNC algorithm and DMT system without clipping operation, respectively. It is worth noting that the gain of the clipping DMT system with CNC algorithm is influenced by both the optimal clipping ratio of clipping operation and the triggered BER value of the CNC algorithm.

5 Conclusion and discussion

In this paper, we investigate a clipping DMT system with the CNC algorithm to improve the performance of PPC IM/DD optical systems. To verify the availability of the CNC algorithm, we conduct an experiment with a 50 Gb/s clipping DMT system using 10G-class commercial devices for the scenario of the PPC PONs. The receiver sensitivity of the clipping DMT system with the CNC algorithm can reach up to −24 dBm at 20% FEC limit, which is 1 and 2.5 dB higher than that of the clipping DMT system without the CNC algorithm and the DMT system without the clipping operation, respectively. Therefore, the superior performance of the clipping DMT system with the CNC algorithm results from the PAPR reduction and clipping-noise mitigation. The error-correction ability of LDPC affects the performance of the CNC algorithm. If the BER after the LDPC decoder equals zero, the clipping noise can be completely mitigated. Therefore, the triggered BER of the LDPC determines the receiver sensitivity of the clipping DMT system with the CNC algorithm. In future work, LDPC with a higher triggered BER

can be designed to achieve superior performance for the CNC algorithm. Notably, the clipping operation and the CNC algorithm are not restricted to their application in the DMT signal, which can also deal with all high-PAPR signals, such as the digital subcarrier modulation and carrierless amplitude/phase modulation.

Acknowledgements This work was supported in part by National Key R&D Program of China (Grant No. 2018YFB1802300), National Natural Science Foundation of China (Grant Nos. 62005102, U2001601, 61971372), Natural Science Foundation of Guangdong Province (Grant No. 2019A1515011059), Guangzhou Basic and Applied Basic Research Foundation (Grant No. 202102020996), Fundamental Research Funds for the Central Universities (Grant No. 21619309), Open Fund of IPOC (BUPT) (Grant No. IPOC2019A001), and Hong Kong Scholars Program (Grant No. XJ2021018).

References

1 Zhou X, Urata R, Liu H. Beyond 1 Tb/s intra-data center interconnect technology: IM-DD OR coherent? J Lightwave Technol, 2020, 38: 475–484
2 Sarmiento S, Mendinueta J M D, Altabas J A, et al. Optical power budget enhancement in 50-90 Gb/s IM-DD PONs with NOMA-CAP and SOA-based amplification. IEEE Photon Technol Lett, 2020, 32: 608–611
3 Le S T, Drenski T, Hills A, et al. 100 Gbps DMT ASIC for hybrid LTE-5G mobile fronthaul networks. J Lightwave Technol, 2021, 39: 801–812
4 Che D, Cho J, Chen X. Does probabilistic constellation shaping benefit IM-DD systems without optical amplifiers? J Lightwave Technol, 2021, 39: 4997–5007
5 Zhou J, Qiao Y J. Low-PAPR asymmetrically clipped optical OFDM for intensity-modulation/direct-detection systems. IEEE Photonics J, 2015, 7: 1–8
6 Wiegart T, Da Ros F, Yankov M P, et al. Probabilistically shaped 4-PAM for short-reach IM/DD links with a peak power constraint. J Lightwave Technol, 2021, 39: 400–405
7 Wunder G, Fischer R F H, Boche H, et al. The PAPR problem in OFDM transmission: new directions for a long-lasting problem. IEEE Signal Process Mag, 2013, 30: 130–144
8 Zhou J, Wang Q, Cheng Q X, et al. Low-PAPR layered/enhanced ACO-SCFDM for optical-wireless communications. IEEE Photon Technol Lett, 2017, 30: 165–168
9 Nissel R, Rupp M. Pruned DFT-Spread FBMC: low PAPR, low latency, high spectral efficiency. IEEE Trans Commun, 2018, 66: 4811–4825
10 Zhang J, Liu Q, Zhu M, et al. Beyond 200-Gb/s/λ DMT signal transmission with NGMI optimization and volterra equalization. J Lightwave Technol, 2021, 39: 5837–5844
11 Zhang L, Hong X Z, Pang X D, et al. Nonlinearity-aware 200 Gbit/s DMT transmission for C-band short-reach optical interconnects with a single packaged electro-absorption modulated laser. Opt Lett, 2018, 43: 182–185
12 Zhang L, Wei J L, Stojanovic N, et al. Beyond 200-Gb/s DMT transmission over 2-km SMF based on a low-cost architecture with single-wavelength, single-DAC/ADC and single-PD. In: Proceedings of European Conference on Optical Communication, 2018
13 Wang W, Zou D D, Wang X W, et al. 100 Gbit/s/λ DMT-PON system based on intensity modulation and heterodyne coherent detection. IEEE Photon Technol Lett, 2021, 33: 1014–1017
14 Pang X D, Ozolins O, Lin R, et al. 200 Gbps/Lane IM/DD technologies for short reach optical interconnects. J Lightwave Technol, 2020, 38: 492–503
15 Le S T, Drenski T, Hills A, et al. High-speed real-time transmissions supporting LTE/5G mobile fronthaul networks using discrete multitone format. In: Proceedings of Next-Generation Optical Communication: Components, Sub-Systems, and Systems X, 2021. 53–60
16 Zou D D, Chen Y C, Li F, et al. Comparison of bit-loading DMT and pre-equalized DFT-spread DMT for 2-km optical interconnect system. J Lightwave Technol, 2019, 37: 2194–2200
17 Bai K, Luo Z B, Zou D D, et al. Quantization noise suppression with noise-shaping technique in DMT-modulated IM/DD optical interconnects utilizing low-resolution DAC. In: Proceedings of Optical Fiber Communication Conference, 2021
18 Tao M H, Zhou L, Zeng H Y, et al. 50-Gb/s/λ TDM-PON based on 10G DML and 10G APD supporting PR10 link loss budget after 20-km downstream transmission in the O-band. In: Proceedings of Optical Fiber Communication Conference, 2017
19 Cimini L J, Sollenberger N R. Peak-to-average power ratio reduction of an OFDM signal using partial transmit sequences. IEEE Commun Lett, 2000, 4: 86–88
20 Jiang T, Yang Y, Song Y H. Exponential companding technique for PAPR reduction in OFDM systems. IEEE Trans Broadcast, 2005, 51: 244–248
21 Wang Y C, Luo Z Q. Optimized iterative clipping and filtering for PAPR reduction of OFDM signals. IEEE Trans Commun, 2010, 59: 33–37
22 Myung H G, Lim J, Goodman D J. Single carrier FDMA for uplink wireless transmission. IEEE Veh Technol Mag, 2006, 1: 30–38
23 Armstrong J. Peak-to-average power reduction for OFDM by repeated clipping and frequency domain filtering. Electron Lett, 2002, 38: 246–247

24 Wang L Q, Tellambura C. A simplified clipping and filtering technique for PAR reduction in OFDM systems. IEEE Signal Process Lett, 2005, 12: 453–456
25 Liu X R, Zhang X Y, Zhang L, et al. PAPR reduction using iterative clipping/filtering and ADMM approaches for OFDM-based mixed-numerology systems. IEEE Trans Wireless Commun, 2020, 19: 2586–2600
26 Chen L, Krongold B, Evans J. Theoretical characterization of nonlinear clipping effects in IM/DD optical OFDM systems. IEEE Trans Commun, 2012, 60: 2304–2312
27 Zhou J, Qiao Y J, Cai Z, et al. Asymmetrically clipped optical fast OFDM based on discrete cosine transform for IM/DD systems. J Lightwave Technol, 2015, 33: 1920–1927
28 Chen L, Krongold B, Evans J. Performance analysis for optical OFDM transmission in short-range IM/DD systems. J Lightwave Technol, 2012, 30: 974–983
29 Chen H, Haimovich A. An iterative method to restore the performance of clipped and filtered OFDM signals. In: Proceedings of IEEE International Conference on Communications, 2003. 5: 3438–3442
30 Zhou J, Sui Q, Li Z. Non-orthogonal discrete multi-tone: toward higher spectral efficiency for optical networks. IEEE Commun Mag, 2021, 59: 70–75